Constructing supramolecular grids: from 4f square to 3d-4f grid

Jian-feng Wu, Lang Zhao, Mei Guo and Jinkui Tang

General Synthetic Considerations. All chemicals and solvents were commercially obtained and used as received without any further purification. IR spectra were recorded with a Perkin-Elmer Fourier transform infrared spectrophotometer. Elemental analysis for C, H, N and S were carried out on a Perkin-Elmer 2400 analyzer.

Ligand H_2L (2,6-bis[(2-pyridylmethylene)hydrazinecarbonyl]-pyridine) was prepared according to a previously published method under ambient conditions. A mixture of pyridine-2,6-dicarbohydrazide (10 mmol) and pyridine-2-carbaldehyde (20 mmol) in 30 mL ethanol was refluxed at 80 °C for 12 h. The solution was cooled to room temperature and the precipitation was filtered and dried in vacuum to give H_2L. Yield: 95 %. Anal. calcd. (%) for $C_{19}H_{15}N_7O_2$: C, 61.14; H, 4.04; N, 26.27. Found: C, 59.98; H, 3.95; N, 26.30. Selected IR (cm^{-1}): 3365.40(br), 3158.12(w), 3050.63(w), 1679.09(m), 1663.89(s), 1587.54(w), 1537.24(s), 1468.75(m), 1437.10(m), 1355.13(w), 1308.21(m), 1265.78(w), 1239.89(m), 1166.97(m), 1078.36(m), 998.85(m), 945.85(m), 843.44(w), 775.93(w), 741.73(w), 643.49(m), 624.18(w).

Ligand H_4L' (2,6-bis[(6-hydroxymethyl-2-pyridylmethylene)hydrazinecarbonyl]-pyridine) was synthesized by the same procedure, using 6-hydroxymethyl-pyridine-2-carbaldehyde to replace pyridine-2-carbaldehyde, in ~ 92% yield. Anal.calcd. (%) for $C_{21}H_{19}N_7O_4$: C, 58.21; H, 4.42; N, 22.63. Found: C, 58.15; H, 4.43; N, 22.51. Selected IR (cm^{-1}): 3375.94(br), 3229.70(w), 1664.71(s), 1586.65(w), 1525.61(s), 1446.35(s), 1342.37(m), 1300.28(m), 1230.49(m), 1157.67(s), 1085.64(m), 1054.43(m), 997.08(m), 944.54(m), 881.09(w), 837.65(w), 797.01(w), 743.81(m), 646.20(br), 613.96(m).

Synthesis of **$[Dy_4L_4(H_2O)_{12}]\cdot(CF_3SO_3)_4\cdot 12H_2O$**, **1**. The reaction of $Dy(CF_3SO_3)_3\cdot 6H_2O$ (0.3 mmol) with H_2L (0.1 mmol) in 5:10 ml methanol/acetonitrile was stirred at room temperature for three hours, then filtrated and left undisturbed, produces colorless crystals of **1** after 9 days in ~ 60% yield. Selected IR (cm^{-1}): 3348.19(br), 1616.07 (s), 1573.95(s), 1556.98(s), 1423.87(w), 1389.34(m), 1374.88(m), 1287.39(m), 1232.23(w), 1218.56(w), 1106.27(w), 1072.89(w), 1041.47(w), 1027.13 (s) 1017.79(w), 938.21(w), 775.49(w), 679.03(w). Anal. Calcd. for $[Dy_4L_4(H_2O)_{12}]\cdot(CF_3SO_3)_4\cdot 12H_2O$ ($C_{80}H_{76}Dy_4F_{12}N_{28}O_{44}S_4$, MW = 3139.92): C, 30.60%; H, 2.44%; N, 12.49%. Found: C, 30.56%; H, 2.35%; N, 12.39%.

Synthesis of **$[Dy_4L_4Cl_4(H_2O)_8]\cdot Cl_8$**, **2**. The reaction of $DyCl_3\cdot 6H_2O$ (0.15 mmol) with H_2L (0.1 mmol) in 5:10 ml methanol/acetonitrile was stirred at room temperature for three hours, then filtrated and left undisturbed, produces colorless crystals of **2**after 7 days in ~ 80% yield. Selected IR (cm^{-1}): 3358.26(br), 1574.38(s), 1557.56(s), 1424.28(w), 1390.67(m), 1375.09(m), 1289.10(m), 1232.43(w), 1218.75(w), 1106.39(w), 1073.27(w), 1041.65(w), 1017.88(w), 938.01(w), 775.28(w), 678.92(w). Anal. Calcd. for $[Dy_4L_4Cl_4(H_2O)_8]\cdot Cl_8$ ($C_{76}H_{76}Cl_{12}Dy_4N_{28}O_{16}$, MW = 2713.05): C, 33.65%; H, 2.82%; N, 14.46%. Found: C, 33.48%; H, 2.76%; N, 14.37%.

Synthesis of **$[Dy_4Cu_4L'_4Cl_8(H_2O)_4]\cdot Cl_4\cdot 28H_2O$**, **3**. The reaction of $DyCl_3\cdot 6H_2O$ (0.2 mmol) with H_4L' (0.2 mmol) and $CuCl_2\cdot 6H_2O$ (0.2 mmol) in the presence of triethylamine (0.4 mmol), with 5:10 ml methanol/dichloromethane as the media was stirred at room temperature for three hours, then filtrated and left undisturbed, produces green crystals of **3** after 7 days in ~ 67% yield. Selected IR (cm^{-1}): 3365.26(br), 1574.65(s), 1557.76(s), 1424.48(w), 1390.87(m), 1374.99(m), 1288.80(m), 1233.73(w), 1219.41(w), 1197.31(w), 1106.45(w), 1073.86(w), 1041.62(w), 1017.93(w), 937.39(w), 774.98(w), 679.75(w), 588.29(w). Anal. Calcd. for $[Dy_4Cu_4L'_4Cl_8(H_2O)_4]\cdot Cl_4\cdot 28H_2O$

($C_{84}H_{132}Cl_{12}Cu_4Dy_4N_{28}O_{48}$, MW = 3631.74): C, 27.78%; H, 3.66%; N, 10.80%. Found: C, 27.75%; H, 3.61%; N, 10.78%.

Crystallography

Single-crystal X-ray data of the titled complexes were collected on a Bruker Apex II CCD diffractometer equipped with graphite-monochromatized Mo-Kα radiation (λ = 0.71073 Å) at 293(2) K. The structures were solved by direct methods and refined by full-matrix least-squares methods on F^2 using SHELXTL-2014. All non-hydrogen atoms were determined from the difference Fourier maps and refined anisotropically. Hydrogen atoms were introduced in calculated positions and refined with fixed geometry with respect to their carrier atoms. Crystallographic data are listed in Table S1. CCDC 1415476-1415478 contain the supplementary crystallographic data for this paper. These data can be obtained free of charge from the Cambridge Crystallographic Data Centre via www.ccdc.cam.ac.uk/data_request/cif.

Magnetic Measurements

Magnetic susceptibility measurements were recorded on a Quantum Design MPMS-XL7 SQUID magnetometer equipped with a 7 T magnet. The variable-temperature magnetization was measured in the temperature range of 1.9−300 K with an external magnetic field of 1000 Oe. The dynamics of the magnetization were investigated from the ac susceptibility measurements in the zero static fields and a 3.0 Oe ac oscillating field. Diamagnetic corrections were made with the Pascal’s constants for all the constituent atoms as well as the contributions of the sample holder.

Arrhenius Plot Fitting.

The temperature and frequency dependence of the magnetic relaxation times for **3** were analyzed in terms of multiple relaxation processes using a reported method (ref. 18).

$$\frac{1}{\tau_{obs}} = \frac{1}{\tau_{QTM}} + AH^2T + CT^n + \tau_0^{-1}\exp\left({-U_{eff}}/{k_BT}\right) \qquad (1)$$

Here, $1/\tau_{\mathrm{QTM}}$ represents the temperature independent quantum tunneling pathway, AH^2T, the direct relaxation process ($\propto T$), CT^n, the Raman relaxation process ($\propto T^n$, n = 4, 5, 7, or 9 typically), and the last term (i.e. the one $\propto \exp(U_{\mathrm{eff}}/k_BT)$), the Orbach process. The best fitted result gives $\tau_0 = 8.1\times10^{-9}$ s, τ_{QTM} = 142.857 s, $AH^2 = 2.37\times10^{-4}$, C = 0.471, n = 8.13, U_{eff} = . 32.2 K.

Table S1. Crystallographic data for complexes **1-3.**

	1	**2**	**3**
Formula	$C_{80}H_{76}Dy_4F_{12}N_{28}O_{44}S_4$	$C_{76}H_{76}Cl_{12}Dy_4N_{28}O_{16}$	$C_{84}H_{132}Cl_{12}Cu_4Dy_4N_{28}O_{48}$
FW, g·mol^{-1}	3139.92	2713.05	3631.74
crystal system	Tetragonal	Tetragonal	Orthorhombic
space group	*I4(1)/amd*	*P4(2)/n*	*Pmmn*
T, K	296(2)	296(2)	273(2)
λ, Å	0.71073	0.71073	0.71073
a, Å	21.384(3)	21.9388(14)	19.3834(15)
b, Å	21.384(3)	21.9388(14)	27.657(2)
c, Å	38.507(6)	16.3350(11)	15.3958(11)
α, °	90	90	90
β, °	90	90	90
γ, °	90	90	90
V, Å^3	17609(4)	7862.2(9)	8253.6(11)
Z	4	2	2
ρ_{calcd}, g·cm^{-3}	1.184	1.146	1.461
GOF onF^2	1.191	1.066	1.731
reflns collected	49084	49144	11904
$R_1{}^{a)}$, wR_2 ($I \geq 2\sigma(I)$)$^{b)}$	0.0993, 0.2983	0.0834, 0.2706	0.1315, 0.3849
R_1, wR_2 (all data)	0.1611, 0.3398	1562, 0.3475	0.1819, 0.4487
CCDC number	1415477	1415478	1415476

$^{a)}R_1 = \sum||F_o|-|F_c||/\sum|F_o|$, $^{b)}wR_2 = [\sum w(F_o{}^2-F_c{}^2)^2/\sum w(F_o{}^2)^2]^{1/2}$

Table S2 Selected bond distances (Å) for complexes **1**, **2** and **3**.

Compound **1**			
Dy(1)-O(2)	2.359(9)	Dy(1)-N(2)	2.508(9)
Dy(1)-O(3)	2.422(8)	Dy(1)-N(1)	2.570(9)
Dy(1)-O(1)	2.430(13)	Dy(1)-Dy(1)#1	11.039(7)
N(1)-O(3)	4.432(1)	N(3)-N(3) #1	4.447(9)

#1 y-1/4, x+1/4, -z+7/4

Compound **2**			
Cl(1)-Dy(1)	2.710(3)	Dy(1)-N(2)	2.528(10)
Dy(1)-O(4)	2.390(10)	Dy(1)-N(5)	2.555(12)
Dy(1)-O(3)	2.391(12)	Dy(1)-N(6)	2.558(11)
Dy(1)-O(1)	2.416(8)	Dy(1)-N(1)	2.583(13)
Dy(1)-O(2)	2.415(9)	Dy(1)-Dy(1)#1	11.172(9)
N(1)-O(1)	4.428(8)	N(3)-N(7)	4.615(2)

#1 –x+1/2, -y+1/2, z

Compound **3**			
N(1)-Dy(1)	2.477(9)	Cl(1)-Cu(1)	2.373(7)
N(8)-Dy(1)	2.467(8)	Cl(2)-Cu(1)	2.362(9)
Dy(1)-O(2)	2.358(11)	Cl(3)-Cu(2)	2.308(6)
Dy(1)-O(5)	2.388(10)	Cl(4)-Cu(2)	2.442(9)
Dy(1)-O(3)	2.390(10)	Cu(1)-N(4)	1.911(19)
Dy(1)-O(4)	2.441(10)	Cu(1)-N(3)	2.069(15)
Dy(1)-O(1)	2.463(12)	Cu(2)-N(5)	1.926(15)
Dy(1)-N(7)	2.453(16)	Cu(2)-N(6)	1.985(16)
Dy(1)-N(2)	2.450(14)	Dy(1)-Cu(1)	5.359(4)
Dy(1)-Dy(1)#1	10.659(6)	N(8)-O(3)	4.327(3)
N(6)-N(6)#1	3.888(6)		

#1 –x+2, y-1/2, -z+2

Table S3 The*CShM* values calculated by *SHAPE* 2.1 for **1**, **2** and **3.**

Central atom	Coordination Geometry	Complex **1**	Complex **2**	Complex **3**
Dy	Triangular cupola (C_{3v})	14.854	14.885	14.450
	Capped cube (C_{4v})	10.263	10.302	9.872
	Capped square antiprism (C_{4v})	1.448	1.417	1.812
	Tricappedtrigonal prism (D_{3h})	1.131	1.301	1.987

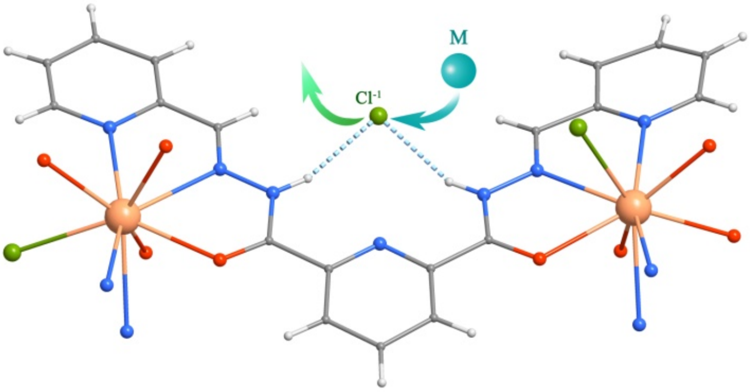

Scheme S1 Schematic drawing of the construction of 3d-4f grid like compound.

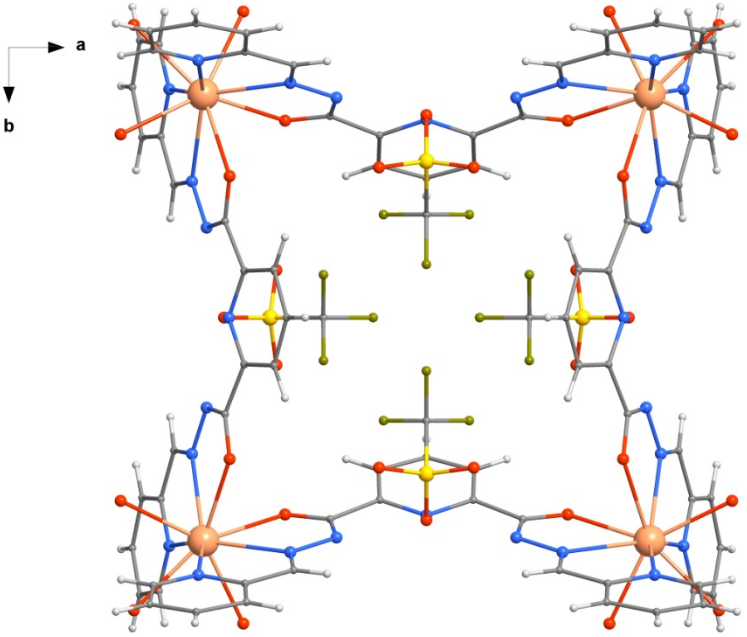

Fig. S1 Structure of **1** with orange, azure, yellow, blue, dark and red spheres representing Dy, Cu, S, N, C and O, respectively; solvents have been omitted for clarity.

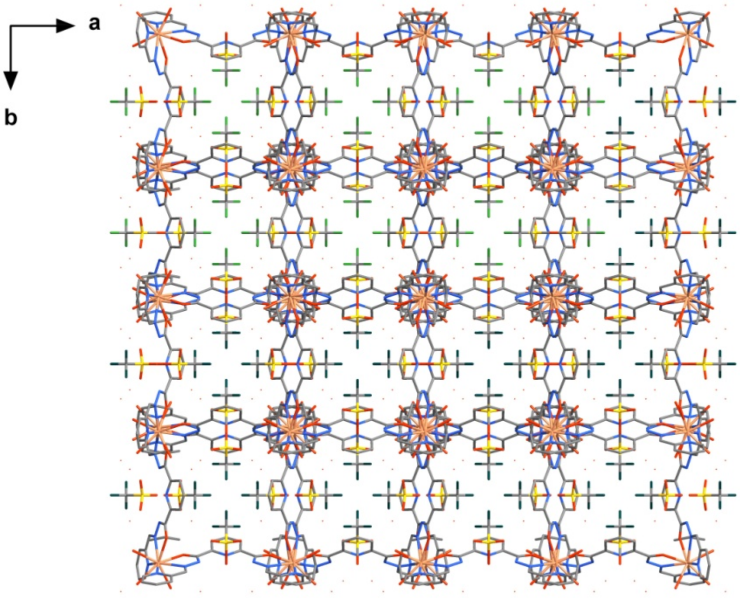

Fig. S2 Packing model of compound **1** along *c* axis.

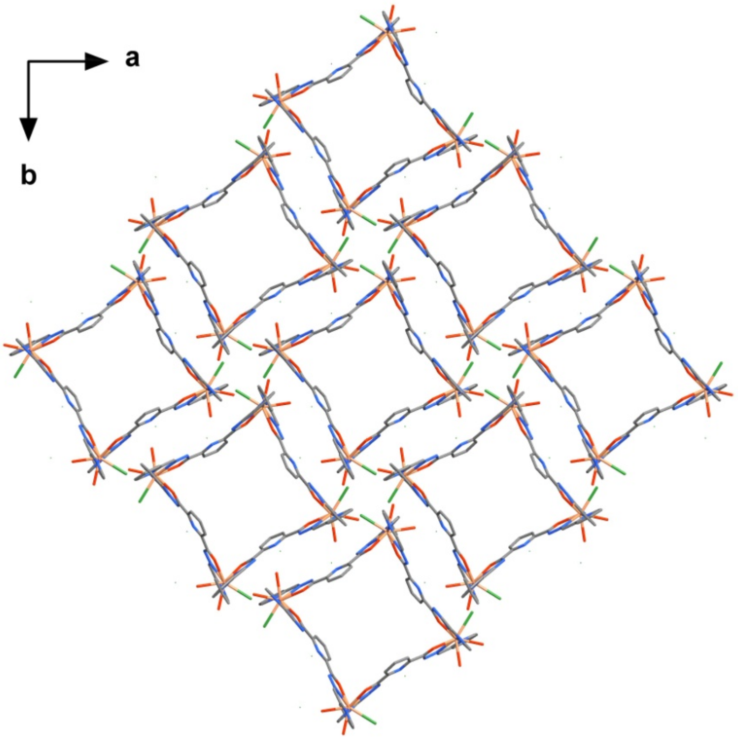

Fig. S3 Packing model of compound **2** along *c* axis.

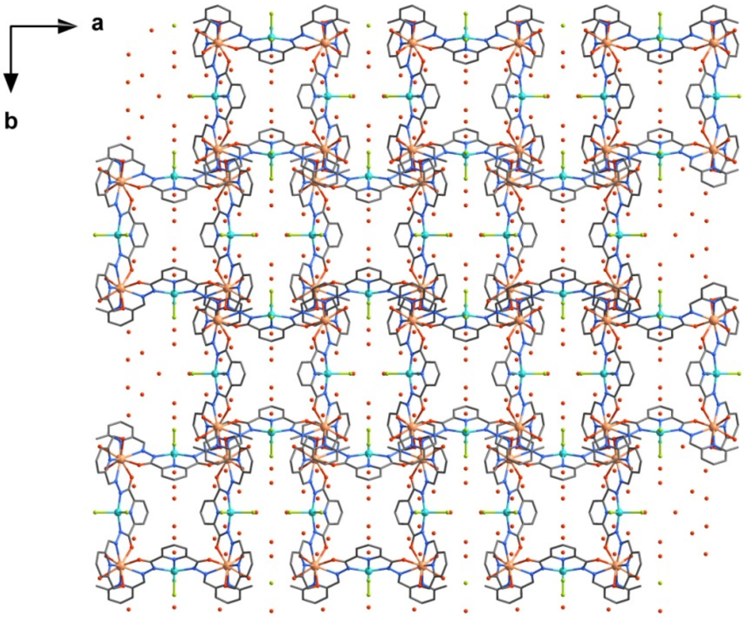

Fig. S4 Packing model of compound **3** along *c* axis.

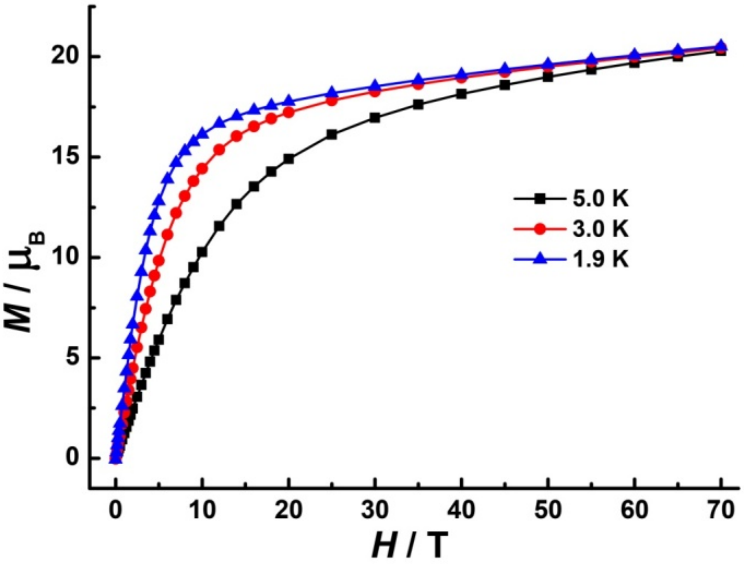

Fig. S5 Molar magnetization (*M*) *vs*. magnetic field (*H*) for **1** at 1.9, 3.0, and 5.0 K.

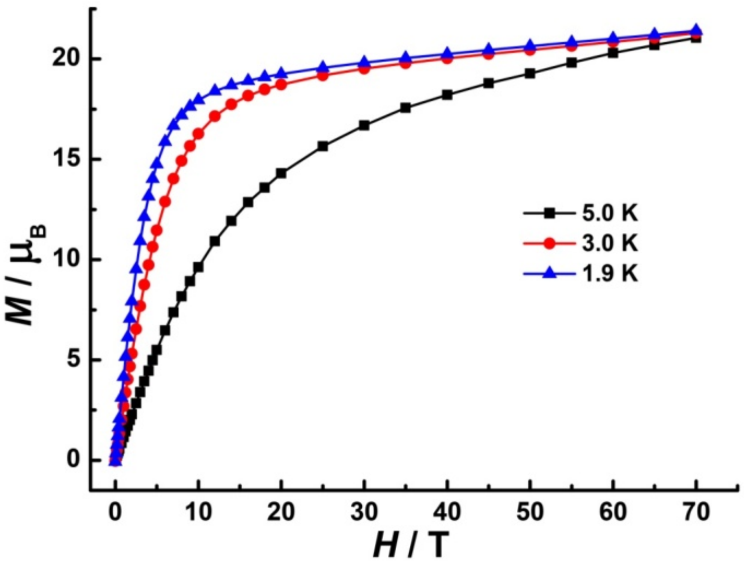

Fig. S6 Molar magnetization (*M*) *vs*. magnetic field (*H*) for **2** at 1.9, 3.0, and 5.0 K.

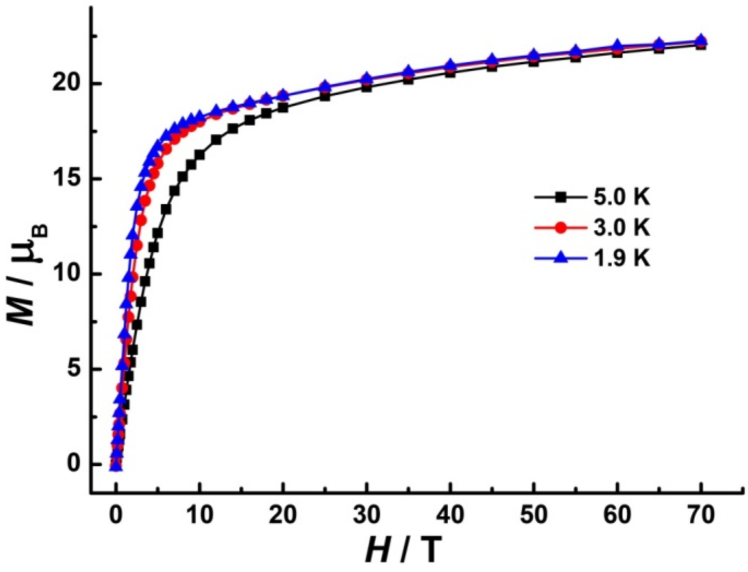

Fig. S7 Molar magnetization (*M*) *vs*. magnetic field (*H*) for **3** at 1.9, 3.0, and 5.0 K.

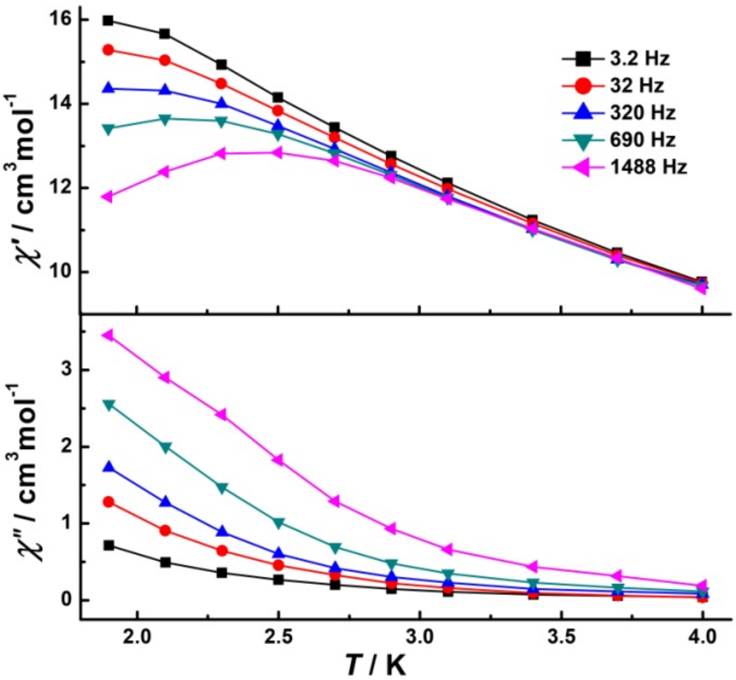

Fig. S8 Temperature-dependent magnetic susceptibilities for **1** at indicated temperatures, under 700 Oe dc field.

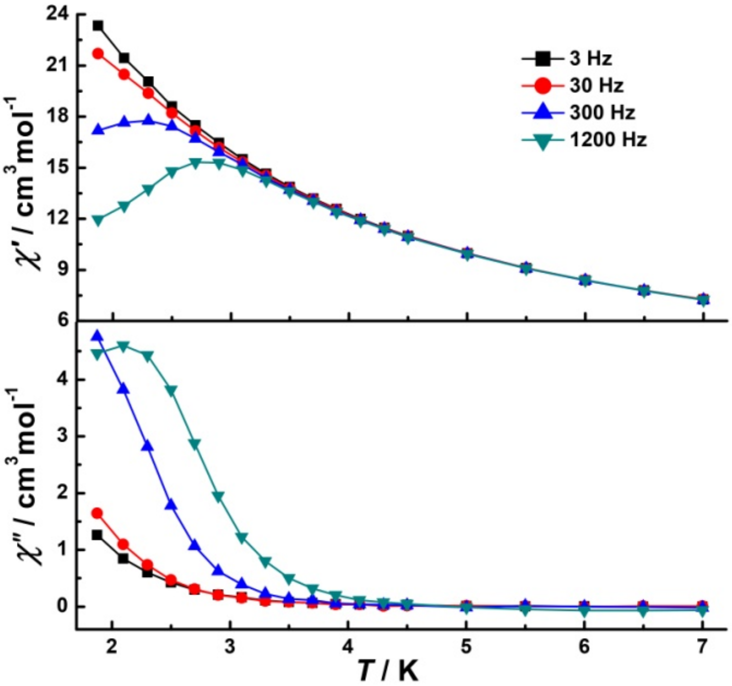

Fig. S9 Temperature-dependent magnetic susceptibilities for **2** at indicated temperatures, under 500 Oe dc field.

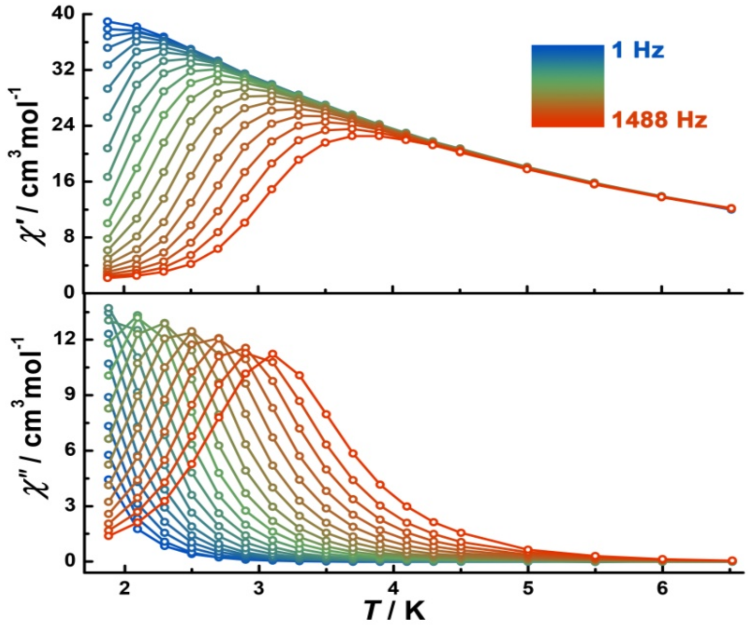

Fig. S10 Temperature-dependent magnetic susceptibilities for **3** at indicated temperatures, under zero dc field.

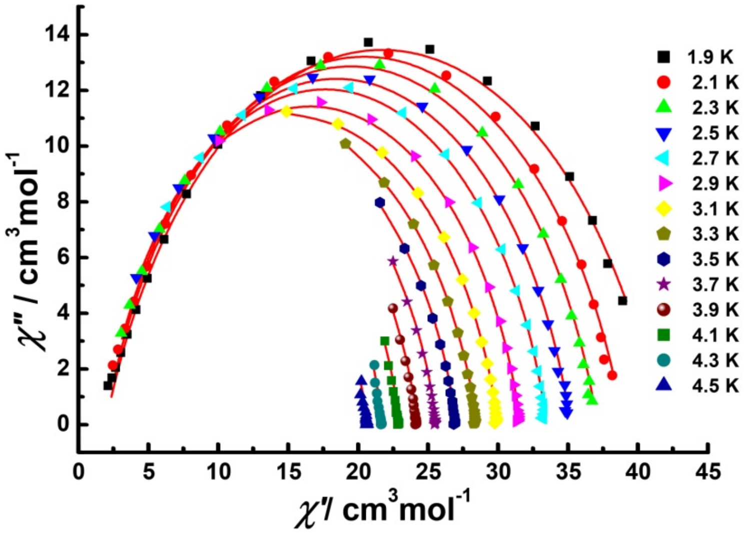

Fig. S11 Cole-Cole plots for **3** at zero field between 1.9 and 4.5 K. The solid lines indicate the best fits to the experiments with the generalized Debye model.

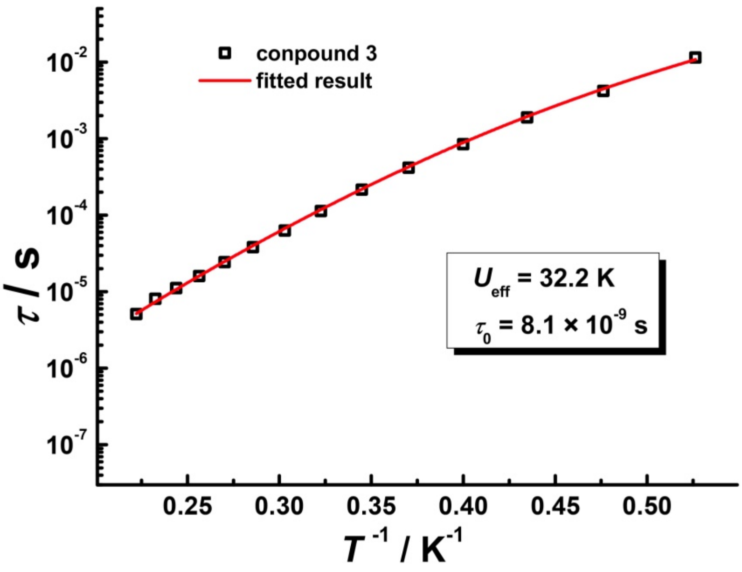

Fig. S12. Plot of τ versus T^{-1} for **3**, obtained under zero fields over the temperature range 1.9–4.5 K. The red line represents the best fitted result.